

# *Garcinia mangostana* A Comprehensive Overview of Ethnomedicine, Phytochemistry, Toxicological and *in Silico* Analysis

Thyagarajan Rajendran <sup>1</sup>, Prakash Pandurangan <sup>1</sup>, Ramesh Kumar Varadharajan <sup>1</sup>, Akshaya Pannerselvam <sup>1</sup>, Narendrakumar Gopakumaran <sup>1,\*</sup>

<sup>1</sup> Department of Biotechnology, School of Bio and Chemical Engineering, Sathyabama Institute of Science and Technology, Chennai, Tamilnadu, India; thyagarajan@gmail.com (T.R.), kpprakashmtech@gmail.com (P.P.), rameshkumar.biotech@sathyabama.ac.in (R.K.V.);

\* Correspondence: gnaren22@gmail.com (N.G.);

Scopus Author ID 56149048200

Received: 27.01.2023; Accepted: 23.02.2023; Published: 2.02.2024

**Abstract:** Ethnopharmacological relevance of *Garcinia mangostana* is a member of the Clusiaceae family distributed in the tropical rainforest of Southeast Asian countries like India, Sri Lanka, Malaysia, and Thailand and also known as "the queen of fruits" due to its extensive treatment ability for abdominal pain, diarrhea, wound infection, chronic ulcer. Parts of the pericarp are extracted with ethanol and fractionated using chromatography for future characterization investigations. For both fractions, phytochemical screening, antioxidant assay, antibacterial assay, and TLC were conducted. The extraction procedure was adjusted by RSM-CCD, and the outcomes were assessed through an antioxidant estimate. DPPH radical scavenging activity was used to determine whether or not both fractions contain antioxidant capabilities. In 89.1 g/ml, the rind extraction was determined to be 69.54 percent. MTT test was used to examine the anticancer activities of HeLa cell lines. The cytotoxicity against normal cells was insignificant since the IC<sub>50</sub> values were 207.07 g/m. The bioactive compounds were evaluated by GC-MS and further used for molecular docking against CDK1- member of the family of cell cycle regulatory proteins involved in the cell cycle maintenance and over-expression of shows association with cancer. The intention of performing docking with the compounds present in the plant extract *in silico* was to establish inhibition of CDK1, which shows the inhibition of cancer.

**Keywords:** *Garcinia mangostana*; ME-GA; phytochemical screening; RSM; MTT; DPPH

© 2024 by the authors. This article is an open-access article distributed under the terms and conditions of the Creative Commons Attribution (CC BY) license (<https://creativecommons.org/licenses/by/4.0/>).

## 1. Introduction

In general, the prevention of a wide variety of cancer is attributable to the presence of bioactive compounds in significant amounts in fruits and vegetables, especially in the waste parts such as the peel and the seeds. Apple peels include phenols, flavonoids, and antioxidants, all of which significantly inhibit the growth of tumor cells [1]. Grape seeds have various health advantages, including anti-inflammatory, anticancer, antiviral, and cardio-protecting qualities [2]. The *Garcinia mangostana* Linn. tree is native to the tropical parts of India that have a rather moderate growth rate. The flesh of the mangosteen fruit is edible and white, and it has a tasty pulp that is sweet and slightly acidic. The external part of mangosteen fruit may be dark purple or reddish in color [3]. After the main edible component of the plant has been consumed, the rinds of the *G. mangostana* plant are often discarded as rubbish. This not only results in the

loss of the plant's bioactive substances but also adds to the untidiness of the surrounding environment [4].

Garcinone E, 8-deoxygartanin, and gartanin are among the considerable amounts of xanthenes found in the fruit's pericarp, along with sitosterol. The rind of the mangosteen fruit has been shown to have significant water-soluble antioxidant [5,6], anti-tumor, anti-inflammatory [7,8], and anti-allergy [6] components.

The activation of cyclin-dependent kinases 1, 2, 4, and 6, which govern the course of the cell cycle, and helps initiate transcription by phosphorylating the C-terminal domain (CTD) of RNA polymerase II (Pol II) at serine 5 (Ser5) at active gene [9]. As preclinical research shows, cancer cells are more dependent than normal cells on high levels of super-enhancer (SE)-driven transcription regulated by certain oncogenic drivers. These oncogenic drivers include RUNX1 in acute lymphoblastic lymphoma (ALL) and N-MYC in neuroblastoma [10]. For the treatment of advanced solid tumors, only four selective CDK7 inhibitors have made it to the Phase I/II clinical study stage [11]. In order to take advantage of the promise of CDK7 inhibitors for use in combination treatments, it is essential to create selective CDK7 inhibitors and understand the mechanism of action these inhibitors have in cancer [12]. Consequently, knowing the function of CDK7 in normal cells as opposed to tumor cells and the underlying mechanisms of CDK7 inhibition in cancer are essential topics of research in medicine and pharmaceutical science [13,14]. This article concentrates on the molecular docking of CDK7 using different compounds derived from the plant source.

In the present study, the pericarp metabolites were extracted, separated, and analyzed for their phytochemical, antioxidant, antibacterial, and cytotoxic activities and their effects on the MCF7 cell line – derived from the pleural effusion of breast adenocarcinoma. The compounds identified using GC-MS were used for molecular docking to understand the interaction with CDK7.

## 2. Materials and Methods

### 2.1. Collection of plant material.

Fresh *Garcinia mangostana* was procured from the local market of Chennai, Tamil Nadu, India. The mangosteen rind was checked for contamination, cleaned to remove dust, and shade dried for 20 days before being crushed into a fine powder. Further, the powder was packed and preserved in the refrigerator until extraction.

### 2.2. Preparation of plant extracts.

Individual parts (rind) were extracted using methanol by homogenization method. After 24 hours of incubation, the extract was filtered using Whatmann No. 1 paper and further concentrated by evaporation. The methanolic extracts were obtained since the samples were absorbed well, used for following tests, and stored at 4°C. It was named ME-GA.

### 2.3. Phytochemical analysis.

The presence of bioactive compounds are identified in the ME-GA of mangosteen by using the procedures described by Kumar *et al.* (2021). Analysis for the presence of carbohydrates, alkaloids, proteins & amino alkanolic acid, theobromine, saponins, glycosides, phytosterols, flavonoids, tannins, and terpenoids was performed [15-17].

2.4. Antioxidant assay.

DPPH solution of 1.1 absorbance at 515 nm was prepared by dissolving approximately 20 mg in 250 mL methanol. A series of different concentrations (50-1000 µg/mL) of standard (gallic acid) and samples were also prepared. The reaction mixtures were prepared by mixing 150 mL of standard and samples with 2850 mL of DPPH radical solution and incubated in the dark at ambient temperature for 24 h. A blank (methanol) and a control (DPPH solution) were also measured at intervals during analysis. The absorbance of the reaction mixtures in triplicate was measured at 515 nm, and for inhibition percentage (% inhibition) calculation, the following equation (1) was used [18].

$$\% \text{ of inhibition} = \frac{A_{\text{Control}} - A_{\text{sample}}}{A_{\text{control}}} \times 100 \tag{1}$$

2.5. Experimental strategy applied using RSM.

One-factor experiments were executed primarily to acquire the optimum state for two parameters while keeping the one parameter persistent. 3 variables, such as time, temperature, and pH, were designated for optimization. Then the impact of three independent parameters (time, temperature, and pH) on the yield of antioxidants was investigated by RSM. This method engages three levels (-1, 0, and +1) of central composite design (CCD) for developing maximum information about the progression from the least number of experiments (Table 1) [19–21].

The design of the experiment (DoE) was formulated with Design Expert software version 7.2.0 (Stat ease Inc. Minneapolis) with the quadratic Eq. (2).

$$Y = v_0 + v_1A + v_2B + v_3C + v_4A^2 + v_5B^2 + v_6C^2 + v_7AB + v_8BC + v_9AC \tag{2}$$

where Y is the obtained response, A, B, and C are the input variables, v<sub>0</sub> is an experimental intercept, v<sub>1</sub>, v<sub>2</sub>, and v<sub>3</sub> are the linear coefficients, v<sub>4</sub>, v<sub>5</sub>, and v<sub>6</sub>, are the quadratic coefficients and v<sub>7</sub>, v<sub>8</sub> and v<sub>9</sub> are the traverse product coefficients with collaboration outcomes.

**Table 1** RSM – CCD Design summary.

Factor	Name	Low		High		Mean	Std. Dev.
		Actual	Coded	Actual	Coded		
A	Temperature	55	-1	75	1	65	8.26343
B	pH	2	-1	4	1	3	0.826343
C	Time	1	-1	3	1	2	0.826343

2.6. TLC analysis.

Thin-layer chromatography (TLC) is used in the process of separating non-volatile substances. In order to put a number on the findings, the distance that is being looked at is divided by the overall distance that the mobile phase has traveled. (The mobile phase must not be allowed to reach the end of the stationary phase) [22].

$$RF = \text{Distance traveled by the solute} / \text{Distance traveled by the solvent}$$

The plates are then removed, dried, and seen under a UV light chamber to view the separated bands.

## 2.7. Anticancer activity by MTT assay.

### 2.7.1. Preparation of cell suspension.

A subculture of MCF7 cells in Dulbecco's Modified Eagle's Medium (DMEM) was trypsinized separately after discarding the culture medium. To the cells in the flask, 25 mL of DMEM with 10% fetal calf serum was added. The cells were suspended in the medium by a gentle passage with the pipette, and the cells homogenized.

### 2.7.2. Seeding of cells.

One mL of the homogenized cell suspension was added to each well of a 24-well culture plate along with doubling the sample concentration (F2) (0 to 200  $\mu\text{g/mL}$ ) concentration and incubated at 37°C in a humidified CO<sub>2</sub> incubator with 5% CO<sub>2</sub>. After 48 hrs incubation, the cells were observed under an inverted tissue culture microscope. With an 80% confluence of cells, a cytotoxicity assay was carried out.

## 2.8. Cytotoxicity assay.

The assay was performed using (3-(4, 5-dimethyl thiazol-2yl)-2, 5- diphenyl tetrazolium bromide (MTT). MTT was cleaved by Succinate dehydrogenase and reductase of viable cells, accommodating a measurable purple product, formazan. This formazan formation is directly comparative to the viable cell number and contrariwise relational to the degree of cytotoxicity. After two days of incubation, the wells were supplemented with MTT and left for 3 hours at room temperature. All wells have removed the content using a pipette, and 100 $\mu\text{l}$  SDS in DMSO was supplemented to dissolve the formazan crystals; absorbance was read in a Bio-Rad plate reader at 570 nm [23].

The IC<sub>50</sub> values were calculated using GraphPad Prism8 by using %inhibition against the corresponding concentration and represented in  $\mu\text{g/mL}$ .

## 2.9. Compound screening by GC-MS.

Gas chromatography-mass spectrometry analysis was carried out with GC-MS-QP2010 Plus Shimadzu. The sample compounds were identified by comparing them to the National Institute of Standards and Technology (NIST) database.

## 2.10. In-Silico studies/Docking calculations.

Six compounds were selected for docking studies, namely,  $\alpha$ -D-mannopyranoside, methyl 3,6-anhydride, phenol, 2-methoxy-4-(1-propenyl)-, (E)-n-Hexadecanoic acid, Nitric acid, nonyl ester, and d-mannitol, 1-O-(22-hydroxydocosyl). The 3D structures of the compounds were downloaded from PubChem as 3D Conformer in sdf format. The energy optimization of these compounds was performed using Maestro - Schrodinger Software by Ligprep application. In addition, each ligand SDF file was produced by utilizing the Maestro ligand preparation wizard in conjunction with the OPLS 2005 force field. This field performed an analysis of a number of probable 3D stereoisomers and protonation states using EpiK. The bioactive chemical conformer with the lowest energy in three dimensions was selected for docking purposes. In the beginning, the 6 compounds and the different protonation states for a few compounds were put through high throughput virtual screening (HTVS) using the OPLS force field. Using the receptor grid generator (Glide) the grid center of the receptor (Mpro) was

defined as the coordinates of the peptide-like inhibitor (X = -5.442, Y = 33.937, Z = -21.307) with specified inner box (30, 30, 30) dimensions. With the ligand docking application to get precise information on the binding postures of these compounds, we put them through standard precision (SP) testing using the OPLS 2005 force field. In addition, Extra Precision sampling (XP) was carried out to get rid of the false positives, and an advanced scoring function was used to validate the binding docking poses. This function enables the inclusion of non-covalent interactions, as well as a penalty for the entropy effect and a penalty for the restriction of ligands. It is referred to as Glide G-score or XP glide score. The optimized structures were docked at the active site of protein CDK1 structures, revealing conserved and unique features of the essential cell cycle CDK. The coordinates of these enzymes were extracted from the crystal structures of these enzymes in Protein Databank RCSB PDB. PDB structure with the code: 4YC6 was used as the Drug-Target Binding Energy was calculated using Schrodinger Software, and subsequently, the calculated binding energy was used to evaluate the stability of the target protein and ligand complexes. PyMol was used to visualize docked inhibitors at the active site and identify the intermolecular interactions with the active site[16,24].

### 3. Results and Discussion

#### 3.1. Extract characteristics.

The characteristics study of extracts of the rind of *Garcinia mangostana* reveals that the methanolic extract of the rind has shown reddish brown. This may be due to the presence of tannins and terpenoids in the rind. The extracts were named ME-GA.

#### 3.2. Phytochemical analysis.

The phytochemical bioactive compounds of ME-GA of *Garcinia mangostana* were qualitatively analyzed, and the results are given in Table 2. Phytochemical screening revealed the presence of carbohydrates, tannins, and terpenoids.

**Table 2.** Phytochemical analysis for crude sample.

S.No	Components	Extract
1	Carbohydrates	++ <sup>1</sup>
2	Alkaloids	+
3	Proteins & A.A	-
4	Theobromine	++
5	Saponins	+
6	Glycosides	-
7	Phytosterols	-
8	Flavonoids	+
9	Tannins	++
10	Terpenoids	++

<sup>1</sup> (++ = highly present, + = moderately present and - = absent)

The result for alkaloids, proteins, theobromine, saponins, glycosides, phytosterols, and flavonoids answered negatively for the extracts, which are supported by the studies of terpenoids are the most important plant pigments for pharmacological applications and natural

flavoring compounds. It is found in ME-GA, which leads us to the conclusion that this may be responsible for the color of the extracts.

The compounds have been separated by column chromatography using silica gel and fractioned compounds (ME-GA1, ME-GA2, etc.). The phytochemical analysis has been analyzed.

### 3.3. Free radical scavenging activity.

Antioxidants act as a defense mechanism that protects against oxidative damage and include compounds to remove or repair damaged molecules [25]. Oxidative stress is a factor for many human diseases as a cause or an effect. Plants are the source of medication for preventive, curative, protective, or promotive purposes [26,27]. Disparity leads to the mutilation of vital biomolecules and organs with possible influence on the organism. Antioxidants can interrupt, constrain or avert the oxidation of materials by scavenging free radicals and waning oxidative stress [28]. Natural antioxidants have been studied extensively for decades to find compounds protecting against several diseases related to oxidative stress and free radical-induced damage.

The effect of given samples on DPPH radical was assessed, rendering to the technique elaborated by [23]. Two mL of  $6 \times 10^{-5}$  M methanolic solution of DPPH were added to 50  $\mu$ l of a methanolic solution (10 mg/ml) of the sample. Absorbance measurements commenced immediately. The results are tabulated in Table 3.

**Table 3.** Antioxidant activity exhibited by the fractioned sample.

S.No	Test sample ( $\mu$ l)	OD	% Inhibition
1.	10	0.538	18.718
2.	20	0.416	46.214
3.	30	0.352	60.648
4.	40	0.272	78.68
5.	50	0.189	97.398

### 3.4. RSM with antioxidant effect.

The optimization using RSM - Central composite design (CCD) was engaged with temperature (A), pH (B), and time (C) were chosen for independent variables. One response was given as antioxidant effect, the value was derived from the polynomial equation (3), and the details are provided in Table 4.

**Table 4.** Design of experiment with the actual and predicted value.

Run	Factor 1 A:Temperature	Factor 2 B:pH	Factor 3 C:Time	AO	
				Actual	Predicted
1	65	3	2	129.5	127.8
2	48.18207	3	2	59.276	56.4
3	65	3	2	129.8	127.8
4	65	3	2	130.2	127.87
5	81.81793	3	2	64.2	65.14
6	65	3	2	127.6	127.8
7	75	4	3	70.5	72.6
8	55	2	3	50.2	52.6
9	55	2	1	58.3	57.44

Run	Factor 1 A:Temperature	Factor 2 B:pH	Factor 3 C:Time	AO	
				Actual	Predicted
10	75	2	1	56.1	55.87
11	65	3	2	119.6	127.8
12	55	4	3	59.2	60.7
13	65	3	2	130.2	127.8
14	75	4	1	53.9	52.7
15	65	1.318207	2	62.3	62.95
16	65	3	0.318207	51.2	51.53
17	65	3	3.681793	66.4	64.23
18	55	4	1	44.9	47.6
19	65	4.681793	2	69.7	67.1
20	75	2	3	59.2	57.82

$$AO = 127.870 + 2.59A + 1.25B + 3.775C + 1.687 AB + 1.6875 AC + 4.4875BC - 23.7158 A^2 - 22.204B^2 - 24.74 C^2 \tag{3}$$

The ANOVA for the model is summarized in Table 5. The F-value and p-value were 174.42 and 0.0001, respectively, both representing the model as significant. The response graph was plotted to understand the interaction of independent variables and confirm the ideal level of each factor for maximum response [29]. Results proposed that the alteration of temperature and pH had noteworthy results ( $p < 0.05$ ). The coefficient of determination ( $R^2$ ) of the models in this response was 0.9936; further, for the predicted model was 0.9766, and the p-value for Lack of Fit was 0.749. These values would give a relatively good fit to the mathematic model in Eq. (3) and are displayed in Table 6. The interaction of different parameters like pH vs. temperature, pH vs. time, and time vs. temperature are shown as a contour plot and surface plot in Figure 1.

**Table 5.** ANOVA.

Source	Sum of Squares	df	Mean Square	F Value	p-value Prob > F	
Model	20579.98	9	2286.664	174.4217	< 0.0001	significant
A-Temperature	91.66282	1	91.66282	6.991839	0.0246	
B-pH	21.63928	1	21.63928	1.650597	0.2278	
C-Time	194.6457	1	194.6457	14.84715	0.0032	
AB	22.78125	1	22.78125	1.737704	0.2168	
AC	22.78125	1	22.78125	1.737704	0.2168	
BC	161.1013	1	161.1013	12.28845	0.0057	
A <sup>2</sup>	8105.48	1	8105.48	618.2682	< 0.0001	
B <sup>2</sup>	7105.132	1	7105.132	541.9639	< 0.0001	
C <sup>2</sup>	8823.941	1	8823.941	673.0709	< 0.0001	
Residual	131.0997	10	13.10997			
Lack of Fit	45.4114	5	9.08228	0.52996	0.7486	not significant
Pure Error	85.68833	5	17.13767			
Cor Total	20711.08	19				

**Table 6.** Regression analysis.

<b>Std. Dev.</b>	3.62077	<b>R-Squared</b>	0.99367
<b>Mean</b>	79.61798	<b>Adj R-Squared</b>	0.987973
<b>C.V. %</b>	4.547679	<b>Pred R-Squared</b>	0.97666
<b>PRESS</b>	483.4038	<b>Adeq Precision</b>	31.34796

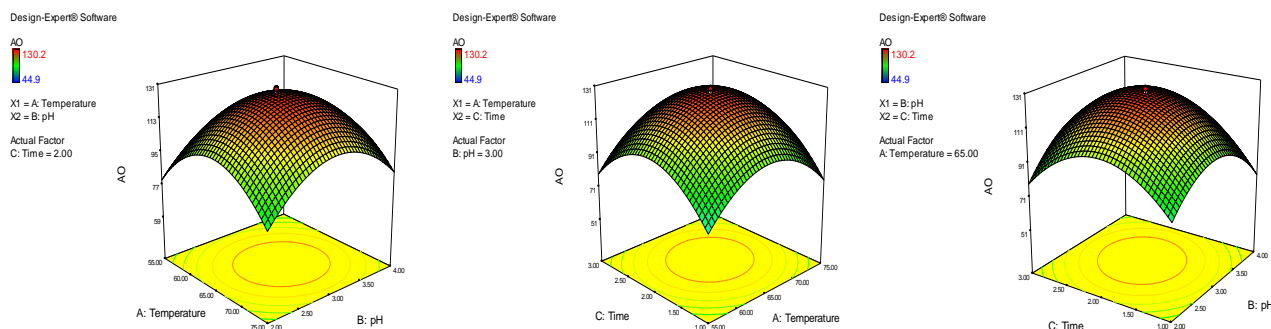


**Figure 1.** Surface and contour plots of different parameters with antioxidants as a response.

3.5. Thin layer chromatography.

TLC analysis of ME-GA3 revealed the presence of active compounds that were visualized in UV. Different solvent systems were tried for each extract to obtain the proper result (Trial and error method). The solvent systems used are tried in different combinations based on the polarity of the compound, as reported by Aziz *et al.*, 2022 [17]. The solvent system used, their ratio, the number of bands obtained, and their RF value is given in the following Table 6.

The standard solvent system tried was ethyl acetate (polar): hexane (non-polar) in the ratio 1:1, for which only the leaf ethyl acetate gave a positive result. The ratio is altered by increasing the hexane solvent with ethyl acetate gave a positive result, but only one bond is formed in that. The other solvent used is methanol which is a polar solvent respectively. The results show that the ME-GA at different proportions of the mobile phase has shown one band.

RF obtained denotes the polarity of the separated bands; larger RF values lower the polarity of the compounds and vice versa. That is, the RF value obtained is inversely proportional to the polarity of the compound.

**Table 6.** TLC results.

Extracts	ME-GA			
	EA: Hex: ET (1:1:1)	Hex: EA (1:2)	Hex: EA (2:1)	Hex: EA (1:1)
Mobile phase	EA: Hex: ET (1:1:1)	Hex: EA (1:2)	Hex: EA (2:1)	Hex: EA (1:1)
RF value	0.5	0.63	0.78	0.43

3.6. Cytotoxicity assay.

The anticancer effect of ME-GA was estimated and shown in Table -7, and Figure 2 depicts the significant cell death of extract against MCF7. 100% of cell death (IC<sub>50</sub> = 27.4±0.74) was seen after a time duration of 72 h.

**Table 7.** MTT activity.

Sample concentration(µg/ml)	% cell viability
0	0
10	32.98 ± 0.33
15	41.98 ± 1.58
20	49.98 ± 1.73

Sample concentration(µg/ml)	% cell viability
25	56.57 ± 1.97
30	60.67 ± 1.46
35	63.64 ± 1.29
40	65.27 ± 1.28
50	69.94 ± 1.15
100	79.02 ± 0.65
150	83.43 ± 0.98
200	88.05 ± 1.09
250	93.4 ± 0.82
300	94.5 ± 0.97
350	96.85 ± 0.78
400	98.1 ± 1.29
450	98.3 ± 0.31
500	98.05 ± 0.32

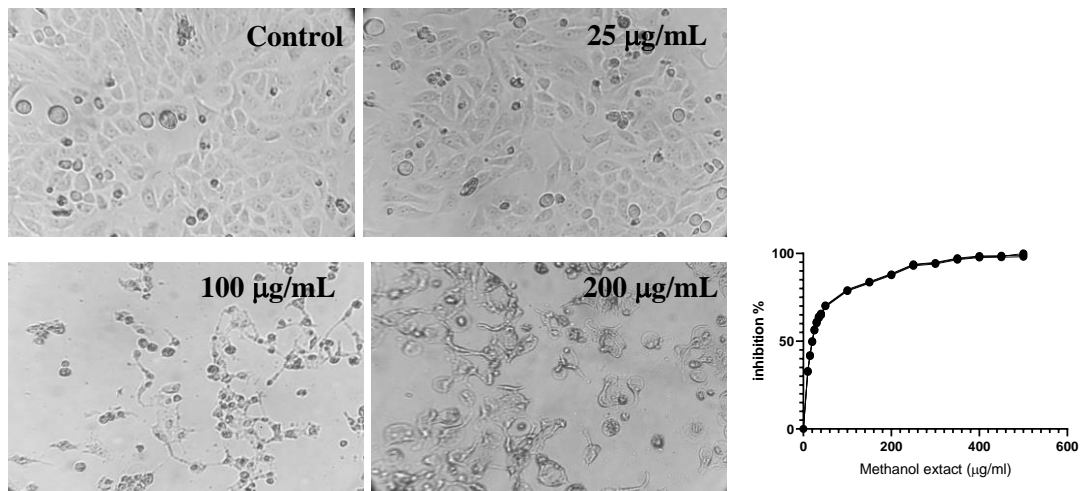


**Figure 2.** MTT.

3.7. Gas chromatography & mass spectrometry.

The GC MS results are shown in Figure 3.

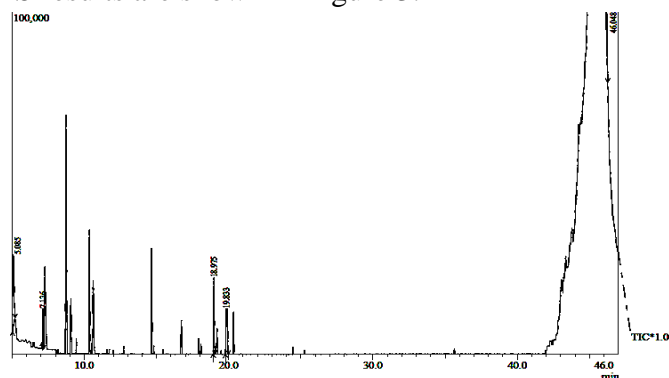


**Figure 3.** GCMS graph.

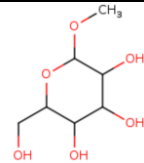
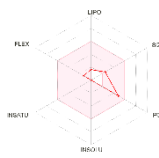
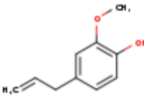
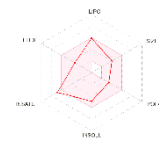
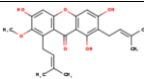
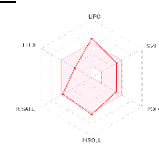
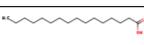
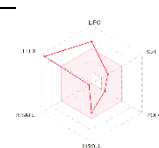
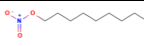
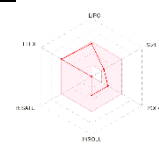
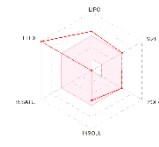
**Table 8.** GCMS analysis for fraction 1.

Peak	R.time	Name	Area	Area %	Height	Height%
1.	5.085	α-D-Mannopyranoside, methyl 3,6-anhydride	126428	9.24	21211	14.68
2.	7.136	Phenol, 2-methoxy-4-(1-propenyl)	33851	2.47	10904	7.55
3.	9.238	α-Mangostin	76509	8.92	41287	21.54
4.	18.975	n-Hexadecanoic acid	69354	5.07	22311	15.45
5.	19.833	Nitric acid, nonyl ester	86592	6.33	13316	9.22
6.	46.048	d-Mannitol, 1-O-(22-hydroxydocosyl)	975724	67.97	35421	31.56

3.8. Drug likeness and ADMET prediction for the components of ME-GA.

Pharmacokinetics and drug-likeness prediction of drug candidate molecules were carried out using the online program SwissADME, which was based on an investigation of ADME. On top of it, there are the rules of Lipinski, Ghose, and Veber, as well as bioavailability scores, were analyzed. The bioavailability score of  $\geq 0.55$  is considered to be significant.

**Table 8.** Drug-likeness results of compounds from GC-MS.

Ligands	2D structure	Graphical representation of drug-likeness	Drug likeness			Bioavailability Score
			Lipinski	Ghose	Veber	
$\alpha$ -D-Mannopyranoside, methyl 3,6-anhydride			Yes; 0	No; 1	Yes	0.55
Phenol, 2-methoxy-4-(1-propenyl)			Yes; 0	Yes	Yes	0.55
$\alpha$ -Mangostin			Yes; 0	Yes	Yes	0.55
n-Hexadecanoic acid			Yes; 1	Yes	Yes	0.85
Nitric acid, nonyl ester			Yes; 0	Yes	Yes	0.55
d-Mannitol, 1-O-(22-hydroxydocosyl)			Yes; 0 violation	Yes	Yes	0.55

**Table 9.** Ligands used in the study and their properties.

Ligands	Formula	Mol.wt (g/mol)	iLogP	TPSA	H bond
$\alpha$ -D-Mannopyranoside methyl 3,6-anhydride	C <sub>7</sub> H <sub>14</sub> O <sub>6</sub>	194.18	1.25	99.38	2
Phenol, 2-methoxy-4-(1-propenyl)	C <sub>20</sub> H <sub>24</sub> O <sub>4</sub>	328.40	4.88	58.92	4
$\alpha$ -Mangostin	C <sub>24</sub> H <sub>26</sub> O <sub>6</sub>	410.46	4.14	100.13	5
n-Hexadecanoic acid	C <sub>16</sub> H <sub>32</sub> O <sub>2</sub>	256.42	3.85	37.30	14
Nitric acid, nonyl ester	C <sub>9</sub> H <sub>19</sub> NO <sub>3</sub>	189.25	2.59	55.05	9
d-Mannitol, 1-O-(22-hydroxydocosyl)	C <sub>28</sub> H <sub>58</sub> O <sub>7</sub>	506.76	5.32	130.61	28

### 3.9. Molecular docking against CDK1.

In the attempt to predict the interaction of different compounds identified by GC-MS with the active sites of CDK1 (PDB code: 4YC6) molecular docking methods were used. The A-chain was used for docking as it showed maximum interaction with the molecules. Other chains were deleted using the prep wizard in pre-processing. There were many active sites, and it ensured an effective reproducibility of results with other compounds also. Thus, docking experiments were conducted to determine the nature of such interaction (Figure 4). Three key amino acid residues (Tyr36, Asp171, and Phe172) of 4YC6 were found to interact directly with compounds of the extract [9-11].

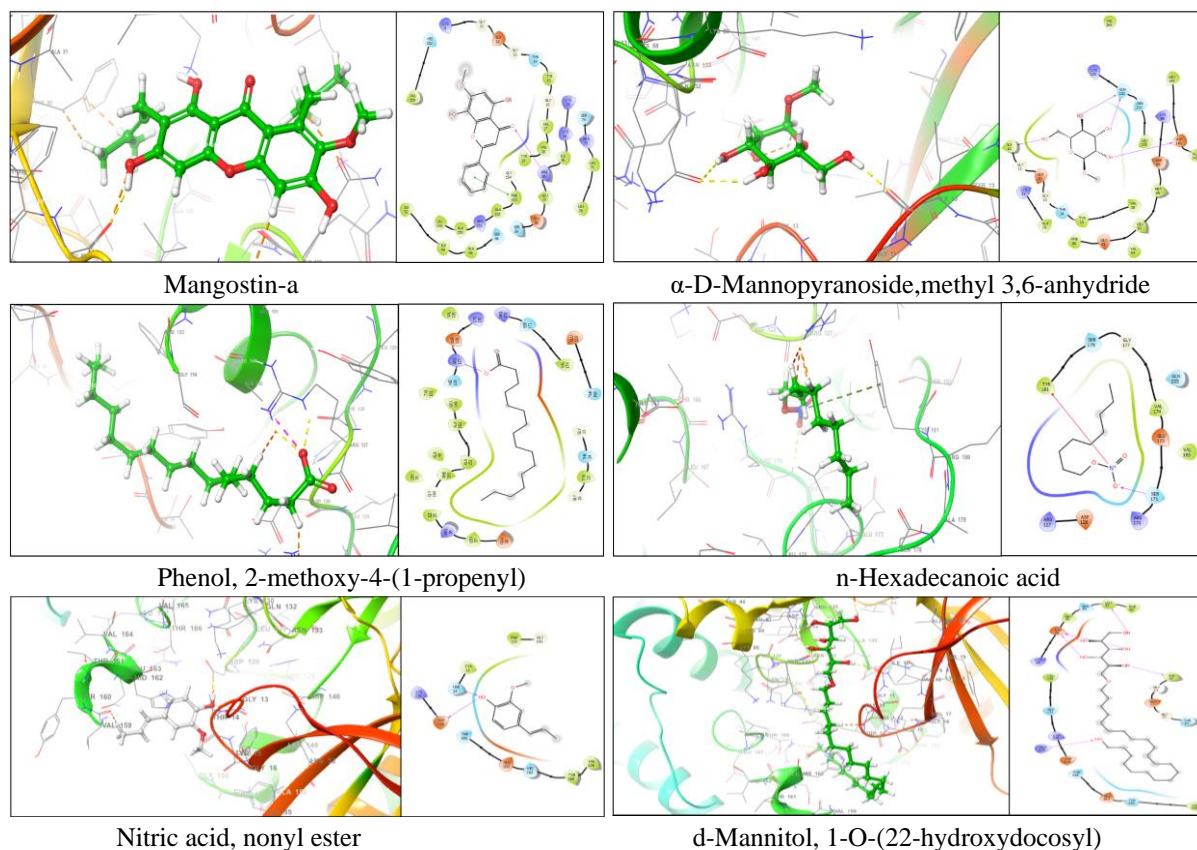


**Figure 4.** Binding orientation of different compounds with protein residues at the active site of 4YC6.

To support the anticancer effect of different compounds against CDK1 and to understand the inhibitory effect, molecular docking was performed. The binding affinity was determined by hydrogen bonding and RMSD score. The binding analysis of the best docking conformation of various compounds is represented in Table 8. Mangostin-a showed interaction with Arg36 and Leu 37 and coordinated covalent bond with phe153; the interaction was present in the binding pocket of CDK1. The overall analysis shows an effective reduction of cancer progression. Similarly, for the other compound, docking was performed against CDK1, and the interactions are shown in Figure 4

### 3.10 $\alpha$ -Amylase inhibition

An additional approach, known as the molecular docking method, was used to understand better how the substance n-hexadecanoic acid might be utilized to block the amylase enzyme. In order to cure or prevent obesity, the protein known as 6BSZ-Human

mGlu8 Receptor Complexed with Glutamate and the component of ME-GA were employed. This helped reduce the amount of glucose absorbed inside the body (Figure 5).

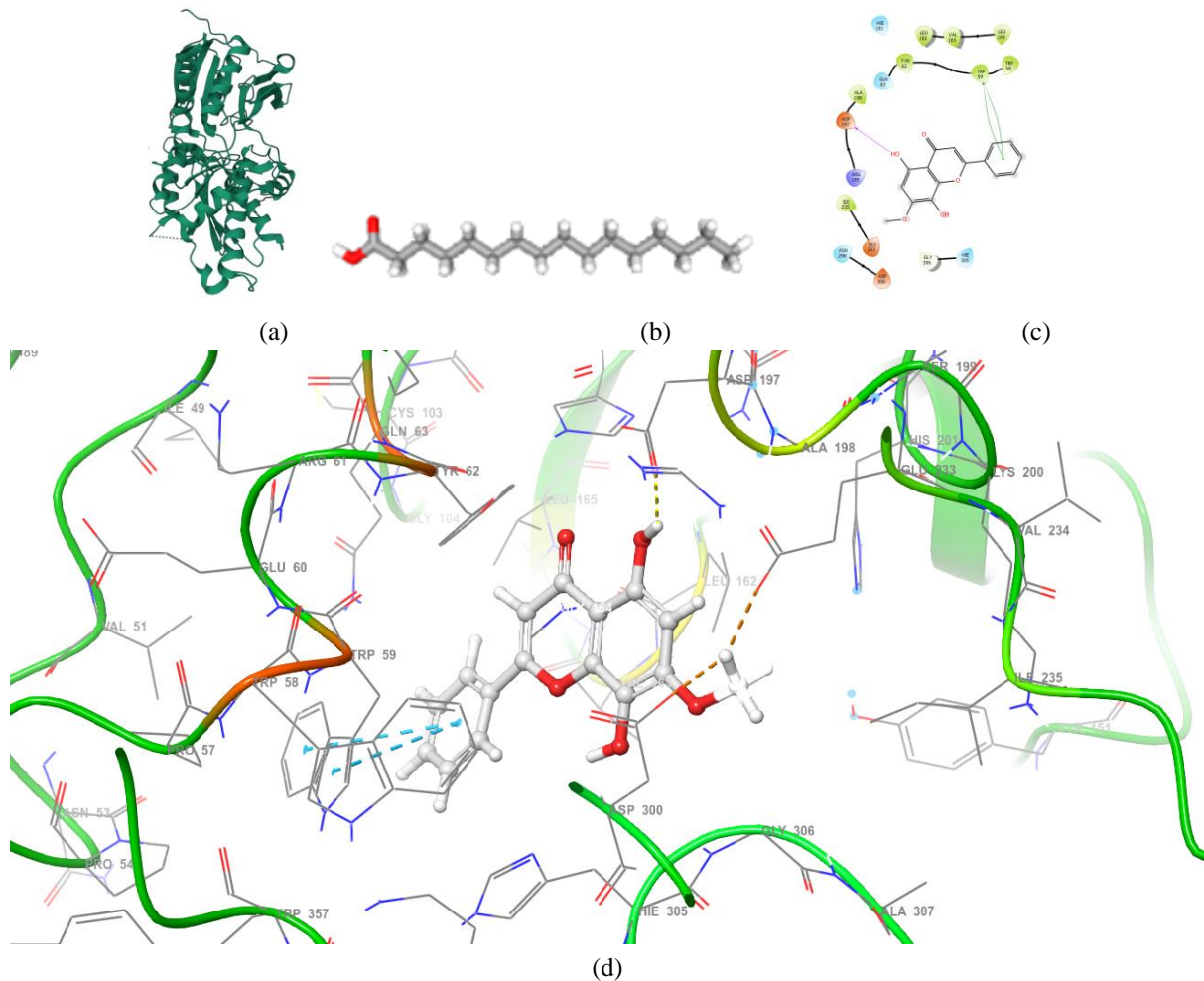


**Figure 5.** (a) Three-dimensional modeling of 6BSZ. (b) Three-dimensional diagram illustrating n-Hexadecanoic acid. (c) Two-dimensional diagram illustrating binding interaction of active conformation of ligand-binding interaction (d) Superimposed three-dimensional structure of ligand (white) with protein (green color) in the active site of  $\alpha$ -amylase.

#### 4. Conclusions

So far, numerous plants have been demanded to pretense beneficial health consequences such as antioxidant properties. Therefore, the current examination was started with the aim of evaluating the free radical scavenging activity of various extracts of *Garcinia mangostana*. The extraction process was optimized using RSM-CCD, and the results were evaluated using antioxidant estimation. The study result reveals that both fractions possess antioxidant properties that were further evaluated by DPPH radical scavenging activity. Rind extraction was found to be 69.57% in 89.1  $\mu\text{g/ml}$ . The anticancer activity assessed in MCF7 cell lines was evaluated by MTT assay. The bioactive compounds were evaluated by GC-MS. Additional molecular docking was done against CDK1 in order to demonstrate how well cancer may be controlled.

#### Funding

This research received no external funding.

## Acknowledgments

The authors thank the Management of the Sathyabama Institute of Science and Technology extended toward completing this work.

## Conflicts of Interest

The authors declare no conflict of interest.

## References

1. Watanabe, C.; Miyata, R.; Wakayama, S.; Kumazawa, S. New acylated flavonoid isolated from Thai bee pollen using molecular networking analysis and determination of its catechol-O-methyltransferase inhibitory activity. *Phytochem. Lett.* **2023**, *53*, 239–244, <https://doi.org/10.1016/j.phytol.2023.01.003>.
2. Wang, L.; Shen, H.; Zhan, Y.; Zhang, Y.; Zhang, Y.; Chen, M.; Li, X.; Zhong, D. Simultaneous quantification of 3',4'-dimethoxy flavonol-3-O-glucoside and its major metabolite in human plasma by LC-MS/MS and its application to a clinical pharmacokinetic study. *J. Pharm. Biomed. Anal.* **2023**, *225*, 115203, <https://doi.org/10.1016/j.jpba.2022.115203>.
3. Tan, J.; Zhang, L.; Xu, H. *Garcinia oligantha*: A comprehensive overview of ethnomedicine, phytochemistry and pharmacology. *J. Ethnopharmacol.* **2023**, *306*, 116130, <https://doi.org/10.1016/j.jep.2022.116130>.
4. Shaikh, R.U.; Meshram, R.J.; Gacche, R.N. An investigation on in vitro anti-inflammatory and antiproliferative potential of isolated Labdane diterpenoids from *Andrographis paniculata* (Burm. f.) wall. Ex nees: An important medicinal plant prescribed in Ayurveda. *Eur. J. Integr. Med.* **2019**, *32*, <https://doi.org/10.1016/j.eujim.2019.100983>.
5. Akissi, Z.L.E.; Yao-Kouassi, A.P.; Magid, A.A.; Koffi, J.M.K.; Voutquenne-Nazabadioko, L. Chemical constituents and antioxidant capacities of *Asparagus africanus* Lam. *Phytochem. Lett.* **2023**, *53*, 22–30, <https://doi.org/10.1016/j.phytol.2022.11.004>.
6. Noshad, M.; Alizadeh Behbahani, B.; Nikfarjam, Z. Chemical composition, antibacterial activity and antioxidant activity of *Citrus bergamia* essential oil: Molecular docking simulations. *Food Biosci.* **2022**, *50*, 102123, <https://doi.org/10.1016/j.fbio.2022.102123>.
7. Singh, P.; Yasir, M.; Shrivastava, R. Ethnopharmacologic screening of medicinal plants used traditionally by tribal people of Madhya Pradesh, India, for the treatment of snakebites. *J. Herb. Med.* **2021**, *29*, 100483, <https://doi.org/10.1016/j.hermed.2021.100483>.
8. Islam, M.A.; Zilani, M.N.H.; Biswas, P.; Khan, D.A.; Rahman, M.H.; Nahid, R.; Nahar, N.; Samad, A.; Ahammad, F.; Hasan, M.N. Evaluation of in vitro and in silico anti-inflammatory potential of some selected medicinal plants of Bangladesh against cyclooxygenase-II enzyme. *J. Ethnopharmacol.* **2022**, *285*, 114900, <https://doi.org/10.1016/j.jep.2021.114900>.
9. Hussain, A.; Hussain, A.; Sabnam, N.; Kumar Verma, C.; Shrivastava, N. *In silico* exploration of the potential inhibitory activity of DrugBank compounds against CDK7 kinase using structure-based virtual screening, molecular docking, and dynamics simulation approach. *Arab. J. Chem.* **2023**, *16*, 104460, <https://doi.org/10.1016/j.arabjc.2022.104460>.
10. Zhang, L.; Chen, C.; Li, X.; Sun, S.; Liu, J.; Wan, M.; Huang, L.; Yang, D.; Huang, B.; Zhong, Z.; *et al.* Exposure to pyrazosulfuron-ethyl induces immunotoxicity and behavioral abnormalities in zebrafish embryos. *Fish Shellfish Immunol.* **2022**, *131*, 119–126, <https://doi.org/10.1016/j.fsi.2022.09.063>.
11. Xia, Y.; Jiang, B.; Teng, Z.; Liu, T.; Wang, J.; Aniagu, S.; Zhang, G.; Chen, T.; Jiang, Y. Cx43 overexpression is involved in the hyper-proliferation effect of trichloroethylene on human embryonic stem cells. *Toxicology* **2022**, *465*, 153065, <https://doi.org/10.1016/j.tox.2021.153065>.
12. Thakur, A.; Kumar, A.; Kaya, S.; Vo, D.V.N.; Sharma, A. Suppressing inhibitory compounds by nanomaterials for highly efficient biofuel production: A review. *Fuel* **2022**, *312*, 122934, <https://doi.org/10.1016/j.fuel.2021.122934>.
13. Kumar, A.; Singh, S.K.; Singh, V.K.; Kant, C.; Singh, A.K.; Tripathi, V.; Singh, K.; Sharma, V.K.; Singh, J. An insight into the molecular docking interactions of plant secondary metabolites with virulent factors causing common human diseases. *South African J. Bot.* **2021**, *149*, 1008–1016, <https://doi.org/10.1016/j.sajb.2021.11.010>.

14. Sundarraj, S.; Sujitha, M. V.; Alphonse, C.R.W.; Kalaiarasan, R.; Kannan, R.R. Bisphenol-A alters hematopoiesis through EGFR/ERK signaling to induce myeloblastic condition in zebrafish model. *Sci. Total Environ.* **2021**, *787*, 147530, <https://doi.org/10.1016/j.scitotenv.2021.147530>.
15. Kumari Patial, P.; Sud, D. Bioactive phytosteroids from *Araucaria columnaris* (G. Forst.) Hook.: RP-HPLC-DAD analysis, in-vitro antioxidant potential, *in-silico* computational study and molecular docking against 3MNG and 1N3U. *Steroids* **2022**, *188*, 109116, <https://doi.org/10.1016/j.steroids.2022.109116>.
16. Pandurangan, P.; Shubhasre, P.N.; Pendem, V.N.; Thirunavukkarasu, S.; Senthilrajan, S.; Ravi, S.N.; Gopakumaran, N.; Ravanappan, P. Anti COVID-19 drug - potential bioactive compounds from sprout shoots of *Curcuma longa* rhizome and molecular interaction studies. *Biointerface Res. Appl. Chem.* **2022**, *12*, 4974–4989, <https://doi.org/10.33263/BRIAC124.49744989>.
17. Aziz, M.; Ahmad, S.; Iqbal, M.N.; Khurshid, U.; Saleem, H.; Kashif-ur-Rehman; Alamri, A.; Anwar, S.; Alamri, A.S.; Chohan, T.A. Phytochemical, pharmacological, and In-silico molecular docking studies of *Strobilanthes glutinosus* Nees: An unexplored source of bioactive compounds. *South African J. Bot.* **2022**, *147*, 618–627, <https://doi.org/10.1016/j.sajb.2021.07.013>.
18. Dhas, T.S.; Sowmiya, P.; Kumar, V.G.; Ravi, M.; Suthindhiran, K.; Borgio, J.F.; Narendrakumar, G.; Kumar, V.R.; Karthick, V.; Kumar, C.M.V. Antimicrobial effect of *Sargassum plagiophyllum* mediated gold nanoparticles on *Escherichia coli* and *Salmonella typhi*. *Biocatal. Agric. Biotechnol.* **2020**, *26*, 101627, <https://doi.org/10.1016/j.bcab.2020.101627>.
19. Nisha, J.; Mudaliar, N.; Senthilkumar, P.; Narendrakumar G.; Samrot, A. V Influence of substrate concentration in accumulation pattern of poly(R) hydroxyalkanoate in *Pseudomonas putida* SU-8. *African J. Microbiol. Res.* **2012**, *6*, 3623–3630, <https://doi.org/10.5897/AJMR11.1509>.
20. Arunkumar, T.; Alex Anand, D.; Narendrakumar, G. Production and Partial Purification of Laccase from *Pseudomonas aeruginosa* ADN04. *J. Pure Appl. Microbiol.* **2014**, *8*, 727–731, <https://microbiologyjournal.org/production-and-partial-purification-of-laccase-from-pseudomonas-aeruginosa-ADN04>.
21. Sundararaman, S.; Narendrakumar, G.; Sundari, N.; Amarnath, M.; Thayyil, P.J. Extraction of Pectin from used *Citrus limon* and optimization of process parameters using Response Surface Methodology. *Journal of Pharmacy and Technology* **2016**, *9*, 3618.
22. Narendrakumar, G.; Dhandapani, R. Characterization of aflatoxin B 1 from *Aspergillus* species and biocompatibility studies. *J. Pharm. Res.* **2011**, *4*, 621–623.
23. Thyagarajan, R.; Narendrakumar, G.; Nair, N.; Taskeen, A.; Ramesh kumar, V. Antimicrobial , antioxidant and anticancer activity of kefir extracted from *Pediococcus pentosaceus* strain TNAR03. *IIOAB J.* **2017**, *8*, 87–91, [https://www.iioab.org/IIOABJ\\_8.S2\\_87-91.pdf](https://www.iioab.org/IIOABJ_8.S2_87-91.pdf).
24. Kumar Verma, A.; Kumar, V.; Singh, S.; Goswami, B.C.; Camps, I.; Sekar, A.; Yoon, S.; Lee, K.W. Repurposing potential of Ayurvedic medicinal plants derived active principles against SARS-CoV-2 associated target proteins revealed by molecular docking, molecular dynamics and MM-PBSA studies. *Biomed. Pharmacother.* **2021**, *137*, 111356, <https://doi.org/10.1016/j.biopha.2021.111356>.
25. Gopakumaran, N.; Veerasangili, S.G.; Valliaparambal, P.T. Isolation and characterization of bacteriocins like antimicrobial compound from *Lactobacillus delbrueckii* subsp lactis. *Jordan J. Biol. Sci.* **2017**, *10*, <https://jjbs.hu.edu.jo/files/v10n4/Paper%20Number%201m.pdf>.
26. Kumar, G.N.; Kumar, S.; Vimalan, S.; Prakash, P.; Nandagopal, S.; Kumar, R.B. Optimization of growth promoters on *Desmodium gangeticum* ( 1 ) using RSM- CCD and its antioxidants activity. *Int. J. Pharm. Pharm. Sci.* **2014**, *6*, 2–6.
27. Velázquez-Jiménez, R.; González-Montiel, S.; Sánchez-Ortega, I.; Villagómez-Ibarra, J.R.; Acevedo-Sandoval, O.A. ADMET prediction, Docking, DM analysis and antibacterial screening of epoxy furan-clerodanes from *Croton hypoleucus*. *J. Mol. Struct.* **2023**, *1277*, <https://doi.org/10.1016/j.molstruc.2022.134840>.
28. Vidya, M.; Bano, T.; Velmakanni, R.P.; Merugu, R.; Jayasree, D. Molecular docking and antibacterial activity of some natural products against cariogenic *Staphylococcus aureus*. *Mater. Today Proc.* **2022**, *66*, 496–500, <https://doi.org/10.1016/j.matpr.2022.05.588>.
29. Moharana, M.; Das, A.; Sahu, S.N.; Pattanayak, S.K.; Khan, F. Evaluation of binding performance of bioactive compounds against main protease and mutant model spike receptor binding domain of SARS-CoV-2: Docking, ADMET properties and molecular dynamics simulation study. *J. Indian Chem. Soc.* **2022**, *99*, 100417, <https://doi.org/10.1016/j.jics.2022.100417>.